CrystEngComm

ARTICLE

Controlled synthesis of Truncated Octahedral Bismuth Micron Particles with Giant Positive Magnetoresistance

Longlong Ma,[a, †] Yayang Tian,[a, †] Chao Yang,[a] Yong Li,[a] Zhaoxin Zhou,[a] Yujun Liang,[a] Xike Tian,*[a] and Yanxin Wang[b]

Bismuth with large magnetoresistance (MR) effects depends on crystallinity and grain sizes. In this paper, we report for the first time Bi micron particles (BMPs) with large MR which can be produced with large scale and high quality through a simple low-temperature solvothermal reduction route in highly alkaline media system. Almost all of the BMPs have a very interesting structural characteristic of rounded truncated octahedral shape. In addition, the reaction and growth mechanism of truncated octahedral BMPs have been proposed on the basis of experimental data. It starts with an alkaline media-homogeneous nucleation, and then small crystal nucleus aggregates irregular nanoflakes and assembles to polycrystalline microspheres at the lead of the CTAC soft template and the nucleus is growing at the same time. Then surface recrystallizes happen to form the truncated octahedral bismuth micron particles via Ostwald ripening. Prolong the time, recrystallization continues from the surface to the core in anisotropism. Moreover, the MR of truncated octahedral BMPs can reach up to 130 % at room temperature (T=300 K) and 700 % at temperature T=10 K in the field of 8 T, respectively, with nonhysteretic and quasi-linear field dependence.

Introduction

Bismuth (Bi), which has a rhombohedral structure and semimetallic nature with small carrier effective mass, low carrier concentrations, high carrier mobility and highly anisotropic Fermi surface, exhibits unusual electronic properties.[1-8] Because of its small effective carrier masses (m^*) and long carrier mean free path (l),[1, 4, 9, 10] different morphologies of elemental Bi have been extensively investigated for the giant magnetoresistance (GMR) effects, such as bulk single crystals of Bi,[11] Bi nanowires,[4, 5, 9] Bi thin films[10] and Bi nanoparticles.[12] The controlled synthesis of Bi with larger magnetoresistance has long been a hot research interest among material sciences.[9-12]

High-quality Bi thin films, which keep the largest MR record, have been made successfully by molecular beam epitaxy and electrodeposition.[10, 13] However, they are costly or hard-controlled techniques. Through the investigation, researcher found that the MR of Bi was mainly determined by the carrier mean free path (l). For the free path, which can reach micron size, can be easily regulatory by crystallinity and grain sizes.[10] A further investigative proof of the GMR dependent on the controlled size nanoparticles with high crystallinity had been reported by Wang etc.[12] In summary, high quality micron-sized Bi may have larger MR, while is still lack of directly experimental investigations. For the past few decades, a variety of effective strategies have been carried out to synthesize elemental Bi nanoparticles, including both up-down and down-up processes.[12, 14-23] But there was only one paper which had reported the synthesis of high quality Bi micron-sized particles through a silicon corrosion hydrothermal process, while only the compound of Bi and Si wafer was obtained and the yield of bismuth was low.[16] So, it is quite believed that the high quality micron-sized Bi particles with uniform and well crystalloid will lead to more future advances in bismuth applications.

Herein, we report for the first time Bi micron particles (BMPs) with large MR which can be produced with large scale and high quality through a simple low-temperature solvothermal reduction route in highly alkaline media system. Almost all of the BMPs have a very interesting structural characteristic of rounded truncated octahedral shape with the diameters around 2 μm. In addition, the reaction and growth mechanism of BMPs are proposed on the basis of experimental data. Moreover, the MR of rounded truncated octahedral BMPs with nonhysteretic and quasi-linear field dependence can reach

a. *Address here. Faculty of Materials Science and Chemistry, China University of Geosciences, Wuhan, Hubei, 430074, P.R.China. E-mail: xktian@cug.edu.cn; Fax: +86 27 67884574; Tel: +86 27 67884574*
b. *School of Environmental Studies, China University of Geosciences, Wuhan, Hubei, 430074, P. R. China.*
† Co-first authors, contributed equally to the article.
Electronic Supplementary Information (ESI) available: [details of any supplementary information available should be included here]. See DOI: 10.1039/x0xx00000x

up to 130 % at room temperature (T=300 K) and 700 % at temperature T=10 K in the field of 8 T, respectively.

Results and discussion

Structure and morphology of Bi micron particles (BMPs)

Figure 1 shows the X-ray diffraction (XRD) patterns of synthesized Bi particles. For this result, all the diffraction peaks can be indexed to the standard rhombohedral structure of bismuth (JCPDS No. 05-0519), which belongs to the rhombohedral R-3m point group of elemental Bi. No other related compounds, such as Bi_2O_3 or BiOCl, have been detected.

Figure 2A shows the general FE-SEM image of truncated octahedral BMPs in pH 12.0 systems under 160 °C for 20 h. Most of the BMPs have a very interesting structural characteristic of rounded truncated octahedral shape with the diameters around 2 μm. There are as well as some BMPs even with irregular size. We surmise that the irregular-sized BMPs appeared due to a little of Bi nucleus aggregated into irregular nanoflakes at the initial stage. [24] And the high magnification FE-SEM image of the synthesized elemental Bi, which dispersed on a Si substrate when measured (Figure 2B), further reveals the octahedral shape with rounded surface of a single BMP. Figure 2C shows the TEM image of the products. We can see from the images that the product is solid particle with uniform particle size of about 2 μm. Because of the solid structure, the electron beam of TEM cannot go through the BMP and present dark image. During the SEM observation, EDS was performed to confirm the chemical composition of the sample. The main detectable element by EDS spectra from the sample is bismuth (Figure 2D). The small amount of Si element detected by EDS is from the Si substrate. This point supports the XRD result that the products are quite pure Bi crystals.

Reaction and Growth mechanism of BMPs

In order to prepare the elemental bismuth, Bi(III) salts were intruded into different reaction systems. The common methods were achieved in an acid media by adding acid like HNO_3 aqueous, [25] HCl aqueous, etc., for the reason of restrain the hydrolysis of Bi(III) in the water to the indissoluble complex ion $[Bi_6O_{4+x}(OH)_{4-y}]^{(6-2x+y)+}$ with x=0, 1, 2; y=0, 1, 2, 3. [26-28] On the other hand, if the reductions of Bi(III) salts take place in the homogeneous liquid phase, they will be more easier. If not, the extra strong reductant (e.g. KBH_4, N_2H_4, etc.) should be needed. [12, 29, 30] Based on these approaches, we submitted a new reaction system with a pure organic phase of ethylene glycol (EG) instead of water / organic systems.
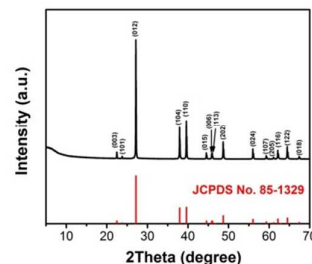

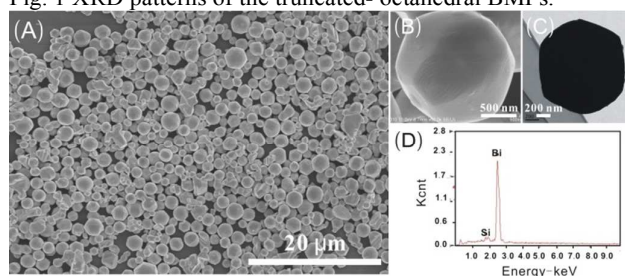Fig. 1 XRD patterns of the truncated- octahedral BMPs.

Fig. 2 SEM, TEM and EDS images of the BMPs with reaction time of 20 h. (A) Low magnification images of the BMPs. (B) Enlarged SEM image of the truncated-octahedral elemental bismuth. (C) TEM image of an individual BMP and (D) EDS spectrum of BMPs.

However, Bi(III) salts as a amphoteric material that had been investigated in the bismuth film electrodes in application of electroanalytical performance in highly alkaline media. [26, 27] They surprisingly found that the Bi^{3+} has no tendency to hydrolysis according to the chemical formula (1) and (2) in highly alkaline media. [26, 27] Another research by Mauro Bertotti explained that a series of hydroxocomplexes may be formed in high pH system, and most of them are soluble except $Bi(OH)_3$. [31] Actually, the Bi(III) is insoluble even at a pH above 13 in the water that probably because of the very low K_{sp} of $Bi(OH)_3$ (4×10^{-31} mol/l). [32]

While EG had been found as a promising solvent for its rather high dielectric constant and also shows high reducibility at high temperatures. So it has been long used for the reduction of Bi(III) salts, but usually acid aqueous were still been added thus forming a component solvent. [19, 20] In a pure organic phase of EG, the highly dielectric constant with very little water may could drive the equilibrium forwards to form soluble component like $Bi(OH)_4^-$, and the experimental phenomena proved it. We found Bi(III) goes through a "precipitate-dissolution" process as the pH raise up to 12.

$$Bi^{3+}+OH^- \rightarrow Bi(OH)^{2+} \tag{1}$$

$$Bi(OH)^{2+} +3e^- \rightarrow Bi+OH^- \tag{2}$$
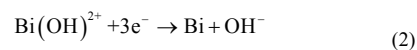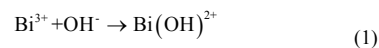
For the starting materials of the reaction were very simple that were much alike the F. FIEVET's theory in the preparation of micron-sized copper and nickel in 1989. [33] So we proposed that the synthesis of this micron particles elemental bismuth could

be also effectively achieved through a polyol process with homogeneous nucleation. According to this theory, ethylene glycol (EG), as a solvent, dissolves the metal salts completely at first. Then EG was dehydrated to acetaldehyde (CH_3CHO), which could reduce the metal complexes to elemental precipitate and then nucleation and growth of metal particles spontaneously in solution. At last, the CH_3CHO was mainly oxidized to diacetyl and the metal complexes were reduced to elemental precipitate at the same time. Possible reaction mechanism of the BMPs synthesis as follows：
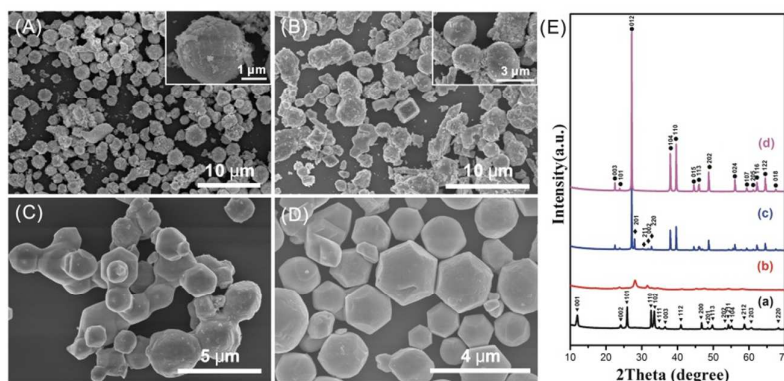

Fig. 3 The effect of different pH on the morphology and component of as-products (Bi/CTAC ratio (1:1), precursor concentration (3 mmol) and reaction temperature (160 ^{o}C)): (A to E) SEM images and XRD patterns of the samples obtained in different initial pH ranges for (A, a) pH= 5-6, (B, b) pH= 8-9, (C, c) pH= 10-11, (D, d) pH= 12-14. The dots, diamonds and triangles represent peaks from bismuth, Bi_2O_3 and BiOCl phases, respectively.
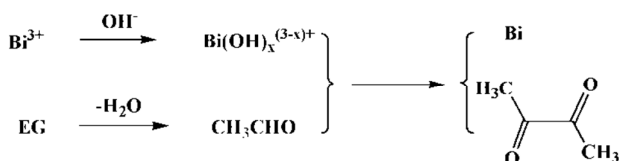
For further understanding of the reaction process of elemental bismuth crystal, experiments were performed by changing reaction conditions, such as the pH, the amount of CTAC and the reaction temperature.

Firstly, we adjusted the pH from 5 to 13 by adding different gram equivalent KOH/EG solution of 0.0375, 0.075, 0.15 and 0.3 g/mL, with other factors (Bi/CTAC ratio (1:1), precursor concentration (3 mmol) and the reaction temperature (160 ^{o}C)) held constant for 20 h. In these conditions, the pH of the initial systems was distributed at a range of 5-6, 8-9, 10-11 and 12-14, respectively. The samples obtained were quite different in component that turned from BiOCl→Bi_2O_3→Bi as determined by PXRD (fig 3E). This means only when the pH above 10, which at least parts of the Bi(III) salt was dissolved, the Bi(III) salt can be reduced to Bi. It shows that only at highly alkaline media, in which the Bi(III) salts can be dissolved completely, the reduction could be completely happen. This may because of that at low pH, the Bi(III) salt were more easy to be surrounded by Cl$^-$ to deposit as BiOCl. At higher pH but below 10, more CH_3CHO contact with the Bi(III) salt which made the reduction can happen, but due to the heterogeneous reaction of interphase
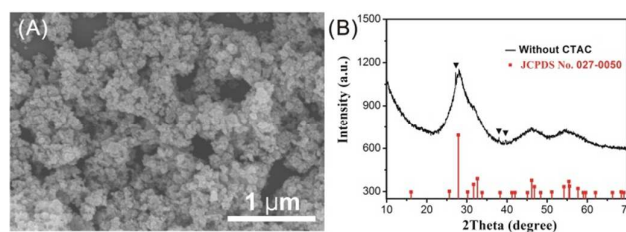

Fig. 4 Sample synthesized in a reaction system without CTAC. A: the SEM image, B: XRD pattern. The triangles represent peaks from bismuth phases.

between the Bi salt and the CH_3CHO that made the reaction activation energy too higher to be fully happen. So when the pH at the range of 8-11, only part of the Bi salts were been reduced. Above pH of 12, all the products turned out to be pure Bi, which attributed to the main contact between Bi salt and CH_3CHO and the lower reaction activation energy of homogeneous phase reaction. However, from the SEM images of the as-products obtained at different pH, the morphologies were only slightly changing and remained the polyhedral micron particles shape. So we proposed the invariance morphology was mainly owing to the CTAC as a soft-template.

To further demonstrate the proposed CTAC effect, we studied the different dosages of CTAC in the reaction systems. When adding CTAC from 0.6 mmol up to 15 mmol into the initial solutions, there was little variation of the products on morphology (figure S1). While as the dosage of the CTAC was 0, the whole morphology, component and structure of as-

products was changed (figure 4). Figure 4A is the SEM image of the sample synthesized in a reaction system without CTAC, it shows very little irregular nanoparticles with size around 25 nm aggregated. The XRD pattern in figure 4B shows that, the
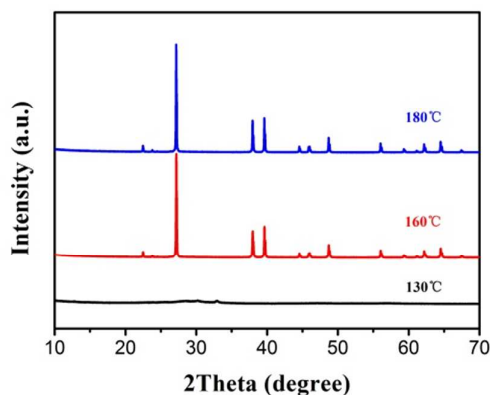

Fig. 5 XRD patterns of samples synthesized with different solvothermal temperatures of 130, 160 and 180 ^{o}C, respectively.
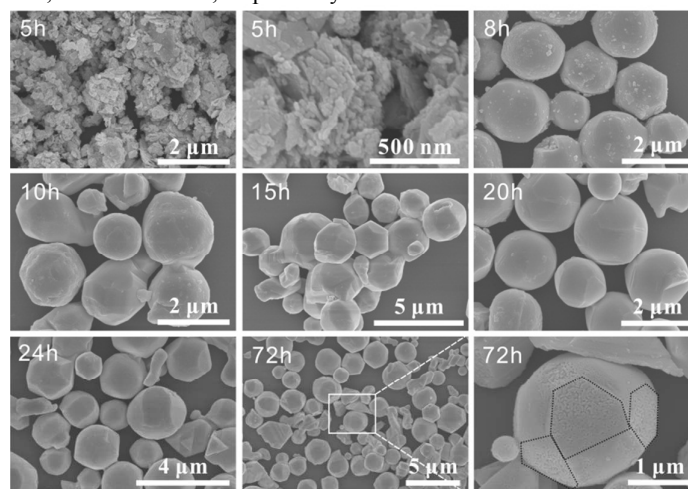

Fig. 6 SEM images of products at different reaction time intervals, from 5 h to 72 h.

as-products were poor crystallinity with Bi/Bi$_2$O$_3$ coexisted at the absence of CTAC in the initial solution. In the overall formation process, the CTAC not only acted as a shape controller, but also facilitated the reduction reaction and obtain high quality and mass produced elemental bismuth.

Besides, the solvothermal temperature was also investigated (see Figure 5). What the influence is mainly the component and crystallization of as-products. It indicated that no reaction happen because there was not any precipitate left at the end of reaction at 130 ^{o}C. After the solution exposing in the air for a few minutes, light yellow precipitate appeared which characterized with poorly crystalline and the mainly diffraction peaks can be indexed to the Bi$_2$O$_2$CO$_3$ (JCPDS No. 41-1488) as shown in Figure S2B. This phenomenon may due to that the Bi(OH)$^{2+}$ which attached on the CTAC templates at the end of reaction subsequently reacted with dissolved CO$_2$ when reaction system exposed in the air. At a higher reaction temperature of 160 ^{o}C, however, the products were transfer to

rhombohedral structure of elemental Bi. Therefore, the elemental Bi can be obtained and exhibits good crystalline in the case of the reaction temperature above 160 ^{o}C.

To study the formation mechanism of the truncated octahedral BMPs, specimens were collected at different intervals of reaction time (at 5, 8, 10, 15, 20, 24, and 72 h) under the reaction temperature of 160 ^{o}C. Figure 6 shows the SEM images of products in the different growth stages. From the FESEM image of the sample produced at 5 h, it can be clearly observed that many irregular nanoflakes which
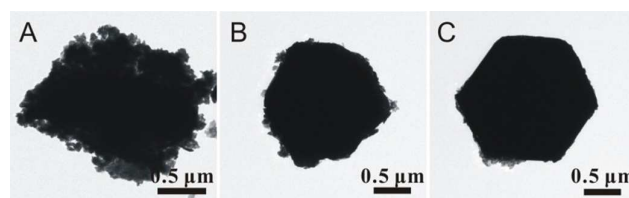
Fig. 7 TEM images of the Bi products collected at different reaction time intervals at (A) 5 h; (B) 6 h; (C) 7 h.

aggregated by small nano crystal nucleus (see the enlarged SEM image of 5 h in figure 6 and figure S3), assembled into microspheres with a typical diameter of about 2 μm. When the reaction time was extended to 8h, the anisotropic micron particles with truncated-octahedral morphology were appeared, and it can be clearly observed that some nanoparticles adsorbed on the surfaces of truncated-octahedral BMPs. From 10 to 20 h, the surfaces of the truncated-octahedral BMPs become smooth and more round in shape. However, as the reaction time increased to 24 h or even to 72 h, the truncated-octahedral BMPs were not turned to sphere, and showed some eroded holes on the surface, which may because of the recrystallization from the surface to the core. The magnification SEM image of the sample (for 72 h) clearly exhibits there are some eroded holes appeared on the surface. Some similar holes can be seen in the as-prepared products at 24 h, we think that the phenomenon evolved to more obviously at 72 h. What is interesting, these holes show order of priority that occurred firstly in the area described by the black dotted line which maybe because of the recrystallization of the truncated-octahedral BMPs with anisotropic structures and different activation energy of different facets. In other words, they took
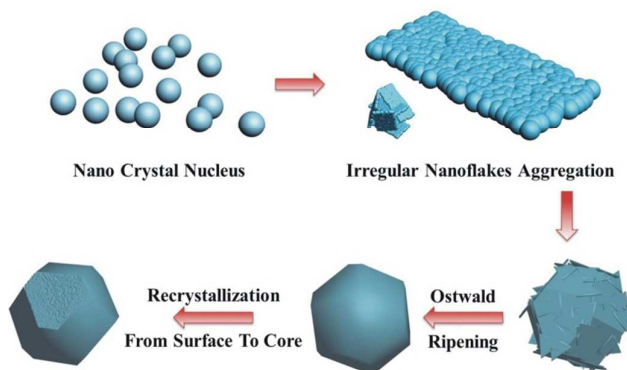

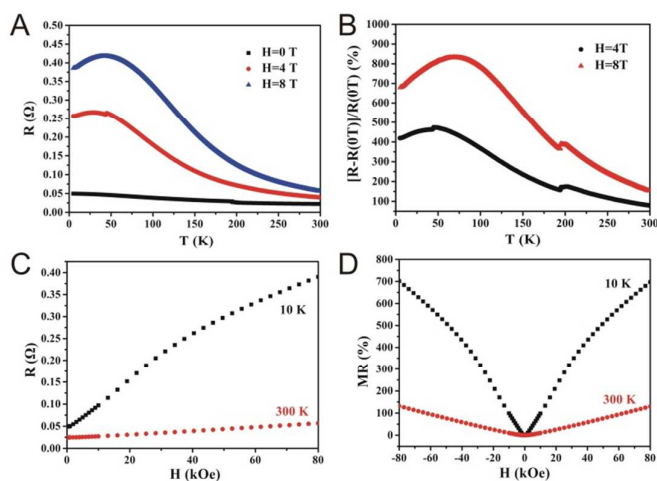Fig. 8 The schematic illustration of the growth process for the truncated octahedral bismuth micron particles.

Fig. 9 Temperature dependence of (A) resistivity and (B) magnetoresistance of the truncated-octahedral BMPs, within magnetic fields of 4 T and 8T; Field dependence of (C) resistivity and (D) magnetoresistance of the truncated-octahedral BMPs at 10 K and 300 K.

place at the higher energy surfaces preferentially. This phenomenon is similar to the crystal process of the zeolite analcime icositetrahedra. [34]

In addition, the period which from nanoflakes at 5 h evolved to preliminary truncated-octahedral BMPs at 8 h were further investigated by the TEM characterization. Figure 7 shows the morphologies of samples collected at the time intervals from 5, 6 and 7 h. During the initial stage at 5 h, the Bi nanoflakes which were with around 5 nm in thickness and irregular shape in width assemble into a micron sized particles. Then, the TEM images of samples from 5 h to 7 h indicated a faster surface ripen process that the irregular nanoflakes on the rough surface were gradually reduce over time during these three hours. We can predict that the surface will turn to ripen until a smooth surface obtained in progress.

Based on the above experimental studies, formation mechanism of the truncated octahedral BMPs is proposed in Figure 8. The growth process can be divided into five stages. It starts with an alkaline media-homogeneous nucleation, and then small crystal nucleus aggregates irregular nanoflakes and assembles to polycrystalline microspheres at the lead of the CTAC soft template. In the meantime, the nucleus is growing. Then surface recrystallizes happen to form the truncated octahedral bismuth micron particle via Ostwald ripening. Prolong the reaction time, the recrystallization process continues from the surface to the core in anisotropism. Furthermore, according to the series experiments and discussion, the truncated-octahedral BMPs with pure component, good crystalline, smooth surface and uniform rounded can be prepared under the condition of pH 12, reaction temperature 160 ^{o}C for 20 h.

The Transportation Property

For the transport measurement of the truncated-octahedral BMPs obtained under pH 12, reaction temperature 160 ^{o}C for 20h, a conventional four-probe method with the sample of lateral dimensions 4 mm by 2 mm and thickness of about 1 mm. The resistivity and their T dependence of truncated-octahedral BMPs were measured firstly, from 300 K to 5 K respectively corresponding to zero field, 4 and 8 T (figure 9A). In zero magnetic field, the resistance R(0) increases with temperature decreasing, from 0.022 up to 0.049 ohm, which means the temperature coefficient of resistance (TCR) is negative and the ratio of resistance at 5 K and 300 K, R (5 K) / R (300 K) is about 2.2. So the BMPs may still in the realm of finite-size effects that with a much longer carrier mean-free path (l) than the particle size. However, it is not an exponential TCR that is characteristic for semiconductors and insulators. [5] Because of the larger grains in truncated-octahedral BMPs, the R(0) is less than the bismuth nanoparticles. [10, 12] In addition, for the sample was made by high press and has an intrinsic particle morphology, the R (H=0) is dominated by grain-boundary

scattering, and the dominant factor is the carrier concentration rather than the carrier mobility. [4, 9, 10, 12]

The R (H = 4 T) and R (H = 8 T) increase rapidly as T decreases from 300 K at first, and reach a maximum at about 30 K for B = 4 T and 42 K for B = 8 T. Such a maximum resembles the bismuth nanowires and Bi films, which also have been found in 100 nm Bi nanoparticles. [4, 9, 10, 12] While in the nanoparticles case, the maximum was shifted to higher temperatures and occurred at larger magnetic field than the truncated-octahedral BMPs. [12] This result can be confirmation of the size quantization and magnetic quantization caused rapid with the increasing of mobility at low temperature. In this case, as the figure 9B shows, the MR is about 153 % and 80 % at 300 K at H = 8 T and H = 4 T, respectively, increasing to about 831 % and 472 % at the maximum as the decreasing of temperature.

Figure 9C, D show the magnetic dependent resistivity and the magnetic resistivity of the truncated-octahedral BMPs at a temperature of 300 K and 10 K. The BMPs show nonhysteretic and do not saturate and quasi-linear field dependence in the field range probed. The MR monotonically increases up to 130 % and 700 % with increasing magnetic field from 0 to 8 T at 300 K and 10 K, respectively.

The positive MR of Bi follows that of typical nonmagnetic metals, which also been called the ordinary MR. It is proportional to the cyclotron orbit $\omega_c\tau$ (ω_c is the cyclotron frequency and τ is the relaxation time). [12] In Bi, the key route to increase the MR is to enlarge the relaxation time (τ), which determined by lengthen the carrier mean free path (l). The large grain size and high quality of electrodeposition-made micron Bi films have been reported as an explanation of its larger MR effect than the films made by evaporation and sputtering. [10] Also it has been used for comparing the difference between 50 nm and 100 nm particles. Herein, our micron-sized, high crystalline Bi microspheres show much longer l and larger MR, which show direct proof that the magnetic quantum size effect of Bi can reach micro size.

Conclusions

In summary, we develop a low-temperature solvothermal method in highly alkaline media to produce large scale, high quality truncated octahedral Bi micron particles (BMPs) for the first time. Truncated octahedral bismuth micron particles were obtained with a particle size around 2 μm. Accordingly, the as-prepared micron-sized, high crystalline truncated octahedral BMPs exhibit much longer l and larger MR, which show directly that the magnetic quantum size effect of Bi can attain micron size. The MR of truncated octahedral BMPs can reach up to 130 % at room temperature (T=300 K) and 700 % at temperature T=10 K in the field of 8 T, respectively. Additionally, the reaction and growth mechanism of BMPs have been proposed on the basis of experimental studies. It starts with an alkaline media-homogeneous nucleation, and then

small crystal nucleus aggregates irregular nanoflakes and assembles to be polycrystalline microspheres at the lead of the CTAC soft template and the nucleus is growing at the same time. Then surface recrystallizes happen to form the truncated octahedral bismuth micron particles via Ostwald ripening. Prolong the time, the recrystallization process continues from the surface to the core in anisotropism. Considering these remarkable achievements together with the low cost, longer carrier mean-free path and larger magnetoresistance, we believe that the truncated-octahedral BMPs will have great potential to meet various magnetic technology demands, such as magnetic field sensing.

Experimental

Chemicals

All chemicals were used as received without further purification, which were of AR grade from the Sinopharm Chemical Reagent Co., Ltd. in this work. Deionized water was used throughout.

Preparation of Bi micron particles

In a typical experiment, 3 mmol Bismuth (III) nitrate pentahydrate $(Bi(NO_3)_3 \cdot 5H_2O)$ and 3 mmol Cetyltrimethylammonium chloride (CTAC) were added to 60 mL of ethylene glycol (EG) with stirring to fully dissolved at room temperature, coded solution A. After then, gram equivalent KOH/EG solution of 3 g/10 mL was added drop by drop to the solution A until the pH adjusted to 12.0. Along with the raise of pH, the system has going through a "suspension-solution" process. Finally, a transparent colourless or light yellow solution was obtained and then transferred into an 80 ml Teflon-lined stainless steel autoclave up to 80 % of the total volume. The autoclave was sealed and maintained at 160 °C for 20 h. After the reaction completed, the autoclave was then allowed to cool down naturally to room temperature, and a brown precipitated powder was obtained. And the supernatant turned light brown with an irritant smell. The powder was filtered and washed with deionized water and absolute ethanol for several times and then dried in a vacuum at 60 °C for 12 h before further characterizations.

Characterization and MR measurement

Powder X-ray diffraction (PXRD) analysis was carried out on a Rigaku D/max-βB diffractometer (Cu Ka X-ray radiation, λ= 0.15432 Å). The field-emission scanning electron microscopy (FE-SEM) measurements were carried out with Hitach-SU8100 equipped with an energy-dispersive X-ray spectroscope (EDS) which was operated at an accelerating voltage of 10 kV. Transmission electron microscopy (TEM) were taken with a JEOL 2000EX (JEOL, Japan) operated at 200 kV. Magnetoresistance (MR) was measured from 5 K to 300 K in magnetic field up to 8 T in physical properties measurement system (PPMS, Quantum Design; 1.8 K ≤ T ≤ 1000 K, 0 T ≤ H ≤ 9 T) in a standard 4-probe method. Before the MR measurement, the sample was pressed into a pellet under a pressure of 20 kg/cm^2.

Notes and references

1 G. E. Smith, G. A. Baraff and J. M. Rowell, *Physical Review*, 1964, **135**, A1118-A1124.
2 Y. F. Komnik, E. Bukhshtab, Y. V. Nikitin and V. Andrievskii, *Soviet Journal of Experimental and Theoretical Physics*, 1971, **33**, 364.
3 N. Garcia, Y. H. Kao and M. Strongin, *Physical Review B*, 1972, **5**, 2029-2039.
4 K. Liu, C. L. Chien and P. C. Searson, P*hysical Review B*, 1998, **58**, 14681-14684.
5 J. Kim, D. Kim, T. Chang and W. Lee, *Applied Physics Letters*, 2014, **105**, 123107.
6 W. Ning, F. Kong, Y. Han, H. Du, J. Yang, M. Tian and Y. Zhang, *Scientific reports*, 2014, **4**, 7086.
7 W. Ning, F. Kong, C. Xi, D. Graf, H. Du, Y. Han, J. Yang, K. Yang, M. Tian and Y. Zhang, *Acs Nano*, 2014, **8**, 7506-7512.
8 M. Tian, J. Wang, W. Ning, T. E. Mallouk and M. H. Chan, *Nano letters*, 2015, **15**, 1487-1492.
9 K. Liu, C. Chien, P. Searson and K. Yu-Zhang, *Applied physics letters*, 1998, **73**, 1436-1438.
10 F. Y. Yang, K. Liu, K. M. Hong, D. H. Reich, P. C. Searson and C. L. *Chien, Science*, 1999, **284**, 1335-1337.
11 J. H. Mangez, J. P. Issi and J. Heremans, *Physical Review B*, 1976, **14**, 4381-4385.
12 J. W. Wang, G. H. Cao and Y. D. Li, *Materials Research Bulletin*, 2003, **38**, 1645-1651.
13 M. Lu, R. Zieve, A. Van Hulst, H. Jaeger, T. Rosenbaum and S. Radelaar, *Physical Review B*, 1996, **53**, 1609.
14 J. Fang, K. L. Stokes, W. L. Zhou, J. Lin and W. Wang, *Chemical communications*, 2001, DOI: 10.1039/b106105b, 1872-1873.
15 Y. Wang and Y. Xia, *Nano letters*, 2004, **4**, 2047-2050.
16 H. Liu and Z. L. Wang, *Journal of the American Chemical Society*, 2005, **127**, 15322-15326.
17 Y. W. Wang, B. H. Hong and K. S. Kim, *Journal of Physical Chemistry B*, 2005, **109**, 7067-7072.
18 G. Cheng, J. Wu, F. Xiao, H. Yu, Z. Lu, X. Yu and R. Chen, *Materials Letters*, 2009, **63**, 2239-2242.
19 J. S. Son, K. Park, M. K. Han, C. Kang, S. G. Park, J. H. Kim, W. Kim, S. J. Kim and T. Hyeon, *Angewandte Chemie*, 2011, **50**, 1363-1366.
20 F. Qin, G. Li, H. Xiao, Z. Lu, H. Sun and R. Chen, *Dalton transactions*, 2012, **41**, 11263-11266.
21 A. L. Brown, P. C. Naha, V. Benavides-Montes, H. I. Litt, A. M. Goforth and D. P. Cormode, *Chemistry of materials: a publication of the American Chemical Society*, 2014, **26**, 2266-2274.
22 F. Dong, T. Xiong, Y. Sun, Z. Zhao, Y. Zhou, X. Feng and Z. Wu, *Chemical communications*, 2014, **50**, 10386-10389.
23 Q. Zhang, Y. Zhou, F. Wang, F. Dong, W. Li, H. Li and G. R. Patzke, *Journal of Materials Chemistry A*, 2014, **2**, 11065.
24 J. Zhang, J Liu, Q. Peng, X. Wang and Y Li, *Chem. Mater.*, 2006, **18**, 867-871.
25 A. R. Rajamani, Udaya Bhaskar Reddy Ragula, Nikhil Kothurkar and Murali Rangarajan, *CrystEngComm*, 2014, **16**, 2032-2038.

26 A. Economou, *TrAC Trends in Analytical Chemistry*, 2005, **24**, 334-340.

27 I. Švancara, L. Baldrianová, E. Tesařová, S. B. Hočevar, S. A. Elsuccary, A. Economou, S. Sotiropoulos, B. Ogorevc and K. Vytřas, *Electroanalysis*, 2006, **18**, 177-185.

28 A. N. Christensen, M. A. Chevallier, J. Skibsted and B. B. Iversen, *Journal of the Chemical Society-Dalton Transactions*, 2000, DOI: 10.1039/a908055d, 265-270.

29 J. Wang and Y. Li, *Advanced Materials*, 2003, **15**, 445-447.

30 Y. Li, J. Wang, Z. Deng, Y. Wu, X. Sun, D. Yu and P. Yang, *Journal of the American Chemical Society*, 2001, **123**, 9904-9905.

31 M. Oliveira Salles, A. P. Ruas de Souza, J. Naozuka, P. V. de Oliveira and M. *Bertotti, Electroanalysis*, 2009, **21**, 1439-1442.

32 Y. Ni, Y. Zhang, L. Zhang and J. Hong. *CrystEngComm*, 2011, **13**, 794-799.

33 F. Fievet, J. Lagier, B. Blin, B. Beaudoin and M. Figlarz, *Solid State Ionics*, 1989, **32**, 198-205.

34 X. Chen, M. Qiao, S. Xie, K. Fan, W. Zhou and H. He, *Journal of the American Chemical Society*, 2007, **129**, 13305-13312.

Graphical Abstract

Controlled synthesis of Truncated Octahedral Bismuth

## Micron Particles with Giant Positive Magnetoresistance

Longlong Ma,[a, †] Yayang Tian,[a, †] Chao Yang,[a] Yong Li,[a] Zhaoxin Zhou,[a] Xike Tian*[a] and Yanxin Wang[b]

[a]*Faculty of Materials Science and Chemistry, China University of Geosciences,*

430074 Wuhan, P.R.China. E-mail: xktian@cug.edu.cn;   Fax: +86-27-67884574;
Tel: +86-27-67884574

[b]*School of Environmental Studies, China University of Geosciences, Wuhan, Hubei,*
430074, P. R. China

*Corresponding author: Xike Tian; E-mail: xktian@cug.edu.cn (Xike Tian).

† Co-first authors, contributed equally to the article.
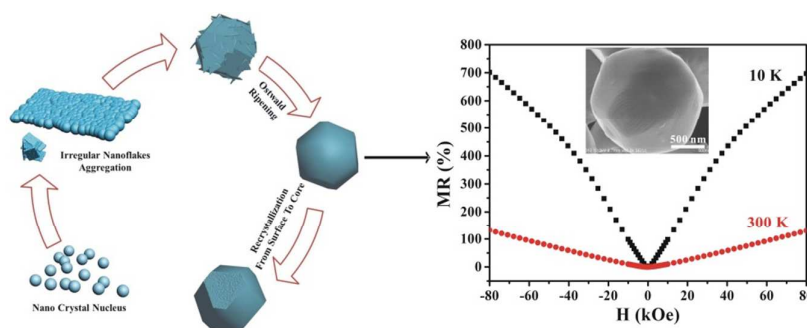
Highlight: Micron-sized truncated octahedral Bismuth crystals with promising giant magnetoresistance (GMR) which can be successfully prepared by a facile solvothermal method in highly alkaline media system for the first time.